

The Relevance of Measurement Systems Analysis

A Procter & Gamble Case Study on
MSA Methodology and Applications

DATE

**OCTOBER
10 AND 12**

TIME

**16:00 CET,
10 am EST**



**CHRISTIAN
NEU**

Scientist
Procter & Gamble



**JERRY
FISH**

Systems Engineer
JMP



**JASON
WIGGINS**


Senior Systems
Engineer
JMP

[Register now](#)

Anna Justen
Christopher Kurth
Gerhard Schaldach
Markus Thommes*

Preparation of Micron and Submicron Particles via Spray Drying and Electrostatic Precipitation

Small particles are of great interest in a variety of applications. Spray drying is a common technique for particle synthesis, but it is limited with respect to sizes below 10 μm . Therefore, a new laboratory-scale spray dryer was designed to address this issue. A novel aerosol generator consisting of a piezo crystal in a swirl chamber was designed to obtain droplets in the low micrometer range. After drying and cooling, particles were deposited in a molten carrier, using melt electrostatic precipitation. The median particle size of three pharmaceutical drug substances was 2 μm . The size distribution was particularly narrow, with span values of about 1.1. Spray drying is a sufficient technique to produce small drug particles below 5 μm with ultrasonic atomization at high frequencies. Electrostatic precipitation in a molten carrier is a suitable method to capture these particles.

 This is an open access article under the terms of the Creative Commons Attribution-NonCommercial-NoDerivs License, which permits use and distribution in any medium, provided the original work is properly cited, the use is non-commercial and no modifications or adaptations are made.

Keywords: Electrostatic precipitation, Micronized particles, Spray drying, Ultrasonic atomization

Received: July 28, 2022; *revised:* September 14, 2022; *accepted:* November 10, 2022

DOI: 10.1002/ceat.202200357

1 Introduction

Several technologies and processes have been developed to produce micron and submicron particles with a narrow size distribution. The desired size depends on the application. For example, in the food industry, the production of microcapsules of functional oils or fatty acids is popular due to the enhanced stability and ability to mask unpleasant taste [1]. In lithium battery technology, a particle size in the upper submicron range is desired for improving electrochemical performance [2, 3]. Nanoparticle production is also of great importance in pharmaceutical applications. Due to the high specific surface area of submicron particles (0.1–1 μm), a high bioavailability is commonly achieved [4]. However, in drug delivery through the lungs, micronized particles (1–10 μm) are desired to avoid exhalation of particles smaller than 1 μm and premature deposition of particles larger than 10 μm in the nose and throat [5]. Micron and submicron particulate systems are known for dust formation, which requires special precautions for their safe handling [6].

To produce these particles, different techniques are used, which can be divided into top-down and bottom-up strategies. Techniques such as dry or wet milling [7, 8] and high-pressure homogenization [9, 10] are known as top-down methods, while supercritical fluid technology and anti-solvent precipitation [11] are bottom-up approaches. One advantage of top-down techniques like milling is the high throughput. But disadvantages are known, such as product contamination by abrasion and high energy consumption [12, 13]. Anti-solvent precipita-

tion is limited by the solvent/anti-solvent system, regarding drug solubility and miscibility of the components [14].

Another well-established bottom-up method is spray drying. It has recently been used for the preparation of micron and submicron particles in many applications [15–17]. It is a continuous process wherein a liquid or a suspension is transformed into particles. Generally, a spray dryer consists of an atomizing unit, a drying unit, and a separation unit [18]. Spray drying is a versatile technique and is used in various applications [19, 20]. Overall, two main challenges arise during spray drying of micron and submicron particles. On the one hand, an appropriate dispersing unit capable of producing small and uniform droplets with high throughput must be found. On the other hand, the recovery of these particles is demanding.

Focusing on dispersion, Strob et al. [21] and Dobrowolski et al. [22] utilized a specially designed pneumatic two-fluid nozzle combined with a droplet-separating cyclone. Large droplets were removed to obtain a higher fraction of small droplets and, hence, submicron particles [21, 22]. Just 1 % of the liquid feed was converted into small droplets. Furthermore, ultrasonic mesh atomizers were also used to generate droplets of 3–15 μm , operating with frequencies of 80–140 kHz [23].

Anna Justen, Christopher Kurth, Gerhard Schaldach, Prof. Dr. Markus Thommes

(markus.thommes@tu-dortmund.de)

TU-Dortmund University, Department of Biochemical and Chemical Engineering, Laboratory of Solids Process Engineering, Emil-Figge-Strasse 68, 44227 Dortmund, Germany.

Submicron particles were produced from aqueous and organic solutions with loads below 1 %, while higher loads tended to clog the mesh atomizer [24–26].

Ultrasonic atomizers are known to generate uniform droplets with high sphericity in gentle dispersing conditions [27]. The droplet size $d_p^{(1)}$ can be predicted according to Lang [28]. It considers properties of the atomized liquid, namely, surface tension σ and density ρ , as well as the ultrasonic frequency f . Rajan and Pandit [27] advanced Lang's approach by adding further properties such as liquid viscosity, flow rate, and energy density within the dimensionless Weber number (We), Ohnesorge number (Oh), and the Intensity number (I_N).

$$d_p = \sqrt[3]{\frac{\pi\sigma}{\rho f^2} [1 + AWe^{0.22} Oh^{0.166} I_N^{-0.0277}]} \quad (1)$$

This approach requires parameters based on experimental data that capture material as well as process properties. Multiple studies were performed to determine the exponents for different liquid systems, ultrasonic frequencies, rheological behavior, and ultrasonic power dissipation [29–32]. Considering Eq. (1), a droplet size in the lower micrometer ($< 10 \mu\text{m}$) region can be obtained with the investigated material at frequencies of about 0.4 MHz.

As mentioned before, the second main challenge in spray drying is the collection of particles in the submicron range. Cyclones are most commonly used, but their high cut-off diameter often leads to incomplete separation of particles below $2 \mu\text{m}$ [5, 33–35]. Wet scrubbing or deep bed filtration are suitable techniques to separate particles. However, the particle recovery of the valuable product is inefficient. Electrostatic precipitation is a more efficient method to collect micron and submicron particles [36–38]. In this method, an electrical potential is applied between a discharge and a collecting electrode, and a corona discharge occurs. The particles are charged via positive or negative polarization and transported in the developed electric field towards the collecting electrode [39].

The aim of this study was to develop a spray dryer that operates with an ultrasonic atomizer consisting of a vibrating piezo crystal. A high excitation frequency was desired to produce particularly small droplets and dried particles (desired range: $0.1\text{--}10 \mu\text{m}$). The dispersing unit and the drying unit were coupled to a custom melt electrostatic precipitator (MESP) [38, 40], allowing them to embed the particles in a hydrophilic carrier material. The performance of this setup was tested with three drug substances, aiming for high drug concentrations in the carrier as well as short process times.

2 Materials and Methods

2.1 Materials

Phenytoin (PTN; Recordati Pharma, Ulm, Germany), naproxen (NPX; Alfa Aesar, Haverhill, USA), and celecoxib (CXB; Hangzhou Yuhao Chemical Technology, Hangzhou, China)

served as drugs in this study, based on their low aqueous solubility, fair toxicity, and their UV traceability. Their high solubility in acetone was beneficial for high throughput in the manufacturing process. Xylitol (Xylisorb 300) was provided as carrier material by Roquette (Lestrem, France) and was used as received. Acetone (Merck KGaA, Darmstadt, Germany), isopropyl alcohol (Carl Roth GmbH & Co. KG, Karlsruhe, Germany), and demineralized water were used as solvents.

2.2 Methods

2.2.1 Preparation

A spray drying apparatus was designed to produce micron and submicron particles by nebulizing a solution (25 g L^{-1}) of the drug substance in acetone with an ultrasonic atomizer (WHQ 3005/1530-12N; Siansonic Technology, Beijing, China) at a frequency of 3.2 MHz. The droplets were transported via carbon dioxide into a drying and condensation compartment (see Sect. 3.1).

The spray-dried particles were collected by electrostatic precipitation. To do this, the drug particles were charged by inducing a negative or positive corona with a high-voltage power supply (Heinzinger PNC 20000-30ump, Rosenheim, Germany). Afterwards, the particles were deflected into a molten xylitol melt with the MESP, which has been described in a previous study [38].

2.2.2 Characterization

The size distribution of the particles was measured prior to precipitation via laser diffraction (Spraytec; Malvern Panalytical, Malvern, UK) using the Mie theory for evaluation. A lens with a focal length of 300 mm was used. The measurement was performed for 30 s, while the average particle size distribution was evaluated. Each determination was conducted in triplicate.

The drug load of the drug substances in the xylitol melt was determined via UV-vis spectroscopy (Jenway 7305, Stone, UK) at a wavelength of 202 nm for PTN, 230 nm for NPX, and 256 nm for CXB, after dissolving in a 1:1 (v/v) mixture of isopropyl alcohol and demineralized water.

The electrical resistivity of the bulk drug material and xylitol in both the molten and crystalline state was determined. The measurements were conducted in a custom-built measurement chamber with a plate-plate electrode arrangement as described in Majid et al. [41]. The sample had a thickness of 3 mm; it was placed between the two electrodes and its electrical resistance was measured at 20 and 120 °C (relative humidity (RH) = 40 %).

3 Results and Discussion

3.1 Spray Drying Process

A piezo crystal (WHQ 3005/1530-12N; Siansonic Technology, Beijing, China) was chosen based on its particularly high resonance frequency of 3.2 MHz and application with organic

1) List of symbols at the end of the paper.

solvents. A high resonance frequency is favorable because of the ability to generate exceptionally small droplets with a narrow size distribution. The atomization with ultrasound is milder with respect to liquid shear compared to the commonly used single- and two-fluid nozzles [27]. An aerosol chamber of about 220 mL volume was designed to use an especially low liquid volume (19 mL) covering the piezo crystal. The drug solution was pumped from a feed tank into the aerosol chamber, and a constant liquid level above the piezo crystal was maintained. Droplets were generated above the liquid surface and transported by carbon dioxide gas, which was fed into the aerosol chamber tangentially. In the resulting vortex, larger droplets were transported towards the walls of the aerosol chamber (Fig. 1).

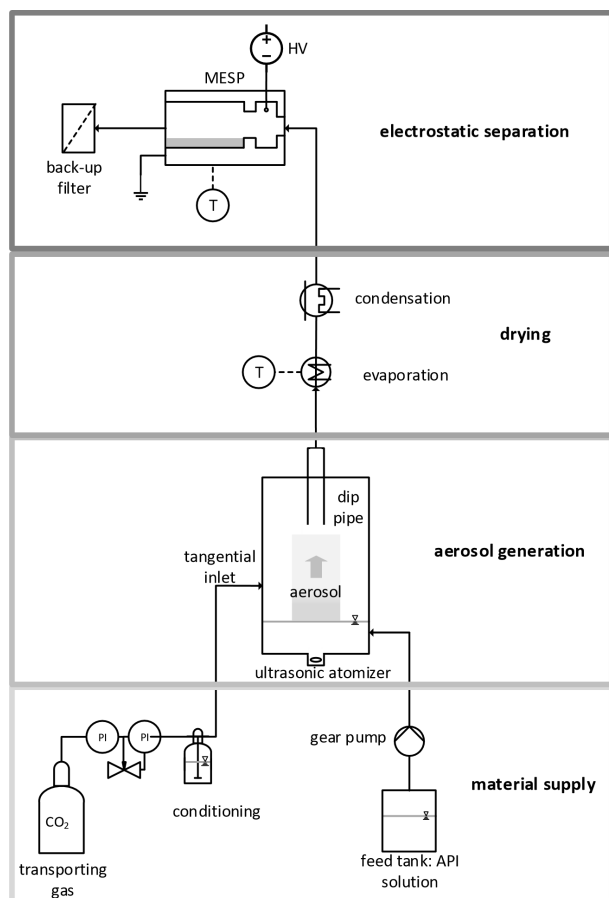


Figure 1. Experimental setup of the aerosol generator combined with the MESP (modified according to [42]). API, active pharmaceutical ingredient; HV, high voltage; PI, pressure indicator.

Small droplets were carried by the gas stream through a dip pipe into the drying unit. In preliminary experiments, precipitation of the solids was observed in the aerosol chamber, which was attributed to rapid droplet drying. The carbon dioxide was taken from a pressurized cylinder possessing a low acetone partial pressure, which was identified as a reason for the drying inside the aerosol chamber. This was overcome using a wash

bottle to enrich the carbon dioxide with acetone before entering the aerosol chamber.

The drying unit consists of a cylindrical ($d = 25$ mm) evaporation and condensation section. The length of the evaporation section was 500 mm, while the condensation section consisted of an intensive condenser of 340 mm in length. Since the transporting gas was heated and cooled without any additional gas stream, the residence time in the different units could be adjusted by the flow rate, while the droplet formation was not affected.

The MESP was developed in a previous study as a two-stage setup [38]. In the first stage, the particles are electrostatically charged by a corona discharge. In the second stage, the particles are deflected towards a collecting electrode, which is covered with molten sugar alcohol. Additionally, a deep bed filter is utilized to minimize environmental contaminations.

This study was performed using PTN, CXB, and NPX as model drug substances, and xylitol as the carrier melt. The liquid level above the piezo crystal and the inlet gas volume flow were identified as relevant process parameters. Different inlet gas volume flow rates were tested, and the lowest flow resulting in a vortex, as observed in the aerosol chamber, was chosen (3.6 L min^{-1}). The droplets were transported into the drying compartment so that dry drug particles emerged to be separated into the xylitol melt in the MESP. The chosen low gas volume flow (3.6 L min^{-1}) led to a higher residence time in the MESP compared to a previous study (120 L min^{-1}) [38], resulting in a higher separation efficiency.

3.2 Particle Size Distribution Measurement

Initial investigations dealt with the droplet and particle size distribution after spray drying using a CXB solution. The droplets were measured prior to and the particles immediately after the drying unit (Fig. 2). The drug particle size was in the desired range ($0.1\text{--}10 \mu\text{m}$), while the submicron particle share was about 10%. Higher standard deviations were observed for droplets than for particles, due to rapid evaporation of acetone during the size determination. Considering the approach of Chan and Kwok [14], a median droplet size of $5 \mu\text{m}$ can be

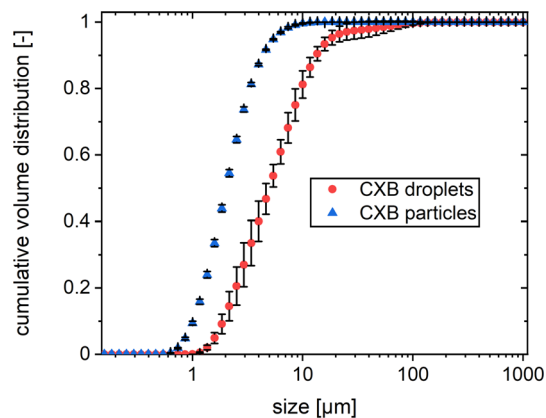


Figure 2. Droplet and particle size distribution of the drug solution of acetone and CXB (CXB droplets) and dried drug particles (CXB particles) ($\bar{x} \pm s$, $n = 10$).

expected to lead to a particle size of about $2\ \mu\text{m}$ when using a solid mass load of 2.5 % in the solution.

A median droplet size of $5\ \mu\text{m}$ is consistent with the approximations in the literature (Eq. (1)), where a droplet size of $2.5\ \mu\text{m}$ is expected. The deviation can be attributed to the lower frequency (20 kHz) used in the literature [27], as well as to size determination issues caused by rapid droplet evaporation. Therefore, a piezo crystal with an excitation frequency in the MHz region is capable of producing micron and submicron particles, which has been proved by Kudo et al. [43] and Yano et al. [44] before. However, there is still a debate about the accuracy of the droplet size distribution in this size range [45].

In further evaluations, particle size distributions of different drug solutions (CXB, NPX, and PTN) were studied (Fig. 3). The volume-based size distributions were found to be similar at median values of about $2\ \mu\text{m}$. A comparatively narrow size distribution was obtained for all drug substances (span = 1.1). Based on these results, the particle size distribution was considered independent of the drug substances used.

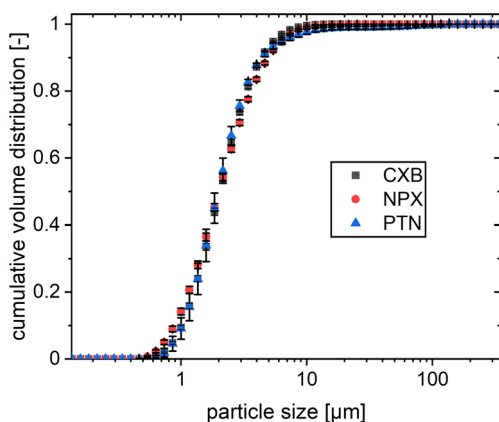


Figure 3. Size distributions of spray-dried particles of CXB, NPX, and PTN, determined by laser diffraction after the drying unit ($\bar{x} \pm s$, $n = 3$).

3.3 Resistivity and Chargeability

One important material property that determines the performance of an electrostatic precipitator (ESP) is the specific resistance ρ_{el} of the particles. Bulk materials with a specific resistance between 10^4 and $10^{10}\ \Omega\text{cm}$ are suitable [40]. Below this value, efficient particle precipitation is difficult due to reentrainment of particles from the deposited particle layer. A specific resistance above $10^{11}\ \Omega\text{cm}$ can cause back-corona effects due to the generation of a strong electric field within the particle layer [46, 47]. To confirm the suitability of the chosen drug substances and the molten carrier (xylitol), the specific resistance was determined in accordance with Majid et al. [41] (Tab. 1).

For the calculation of the specific resistance, the following considerations are necessary. Assuming ohmic behavior of a resistor, the electrical resistance R is equal to the voltage drop ΔU across the resistor divided by the current I through the resistor. Equivalently, R can be expressed in terms of the specific

Table 1. Specific resistance ρ_{el} of PTN, NPX, and CXB with the current density j at the set temperatures T .

Material	Voltage polarization	ρ_{el} [Ωcm]	T [$^{\circ}\text{C}$]
PTN	+	2.2×10^{15}	20
PTN	-	4.4×10^{13}	20
NPX	+	4.5×10^{15}	20
NPX	-	4.1×10^{13}	20
CXB	+	1.8×10^{16}	20
CXB	-	4.5×10^{13}	20
Xylitol melt	+	conducting ^{a)}	120
Xylitol melt	-	conducting ^{a)}	120

^{a)} No electric resistivity measurable due to immediate voltage breakdown.

ic resistance ρ_{el} along with the thickness s and area A_R of a resistive layer such that

$$R = \frac{\Delta U}{I} = \rho_{el} \frac{s}{A_R} \quad (2)$$

The current I divided by the area A_R of the resistive layer is the current density j . Thus, solving for the specific resistance and substituting $1/j$ for A_R/I yields

$$\rho_{el} = \frac{\Delta U}{js} \quad (3)$$

Multiplying both sides of Eq. (3) by the current density leaves the voltage drop ΔU divided by the thickness s of the resistive layer, which is the field strength E inside the layer:

$$E = \rho_{el} j \quad (4)$$

The drug substances (CXB, NPX, and PTN) are highly resistant materials which maintain the charges in the particle layer rather than transporting it to the collecting electrode. This creates a high electric field inside the built-up particle layer, causing particle reentrainment and reducing the precipitation efficiency. This applies to positive and negative polarization, without relevant differences between the three drug substances. The carrier material xylitol was evaluated at process temperature ($120\ ^{\circ}\text{C}$) since it needs to be molten. The measurement of specific resistance was not possible due to high conduction, allowing the xylitol to serve as the collecting electrode.

3.4 Electrostatic Separation

Additional investigations concerning the performance of the MESP were conducted to quantify the operating window. Therefore, the applied voltage was varied systematically. The onset of particle deposition was observed at 5 kV, indicating an operating point above the corona inception voltage for both positive and negative polarization. At higher voltage than

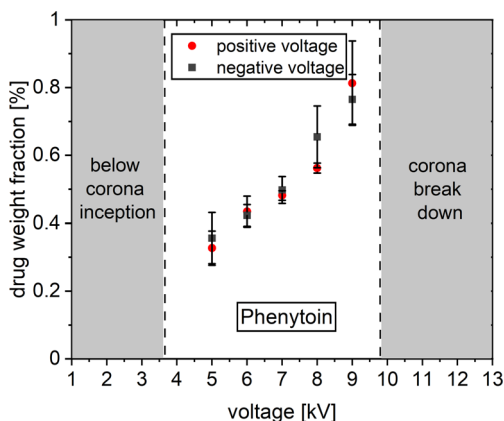


Figure 4. Influence of the voltage at the discharge electrode on the drug load at a constant loading time of 5 min for separated PTN particles for positive (red dots) and negative (grey squares) voltage polarization ($\bar{x} \pm s$, $n = 3$).

9.5 kV, a corona breakdown was observed due to a back-scattering, so that the operating range was defined between 5 and 9 kV (Fig. 4).

The amount of separated drug particles was quantified by the drug concentration found in the xylitol melt after an operating time of 5 min with positive or negative polarization voltage. The drug load increased with the increase of the applied voltage for both negative and positive polarization and all three investigated drug substances (Figs. 4 and 5). Phenytoin weight fractions of up to $0.8 \pm 0.12\%$ were found for the highest applied voltage and a positive polarization (Fig. 3). Generally, a

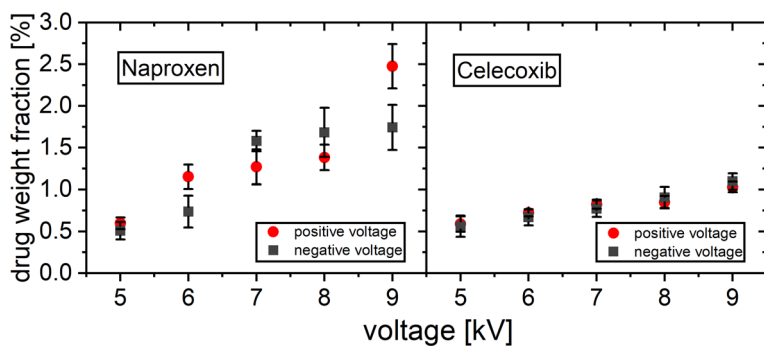


Figure 5. Influence of the voltage at the discharge electrode on the drug load at a constant loading time of 5 min for separated NPX and CXB ($\bar{x} \pm s$, $n = 3$).

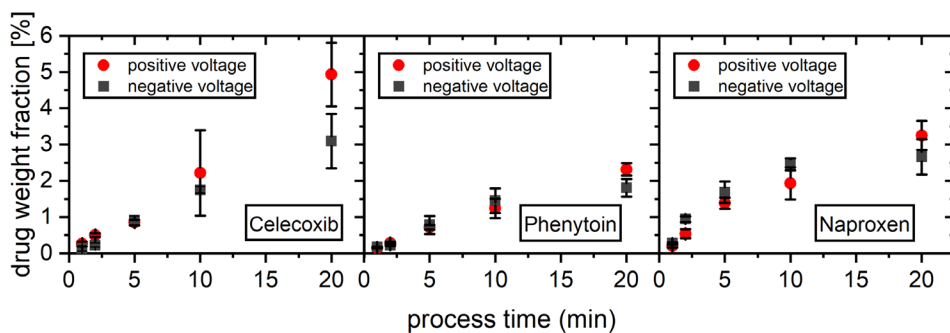


Figure 6. Influence of the process time on the drug load of CXB, NPX, and PTN at constant voltage at the discharge electrode (8 kV) ($\bar{x} \pm s$, $n = 3$).

higher voltage increases the electric field strength; therefore, the particles are separated more efficiently from the gas stream during the comparably short residence time in the MESP [40].

Furthermore, the collected amounts of NPX and CXB (Fig. 5) were quantified at different applied positive and negative corona voltages. Overall, higher NPX contents were found at up to 2.5 wt % for positive voltage polarization (Fig. 5). Since a similar mass flow of drug particles was used, the difference in drug content was attributed to differing electrostatic charging performances of these substances. Moreover, no relevant difference between positive and negative polarization was found.

Further investigations dealt with the influence of the process time on the drug load using a constant voltage of 8 kV with positive and negative polarization (Fig. 6). For all three drug substances, the drug content increased during the process time. CXB and PTN showed a linear correlation, but NPX tended to converge with respect to time. This can be attributed to an insulating particle layer on the surface of the collection material, xylitol. This phenomenon is known in the literature and named back-corona. With increasing layer thickness at the collecting electrode, higher resistance is created – and thereby a higher potential drop in the particle layer [46, 48, 49]. However, much higher drug contents were obtained compared to previous investigations [38]. The differences in drug content between the drug substances were attributed to varying charging performance. With materials like aluminum and silicium oxide [46], ashes [50], or organic compounds [51], it is due to varying electric properties [52]. Differences in the charging behavior of pharmaceutical, inhalable dosage forms were found, but the mechanism was not further analyzed [53, 54]. Pure drug particles have not been investigated yet. Furthermore, there was no relevant difference between the polarization methods.

4 Conclusions

Within this study, an experimental framework was developed and established to produce and collect micron and submicron drug particles using spray drying and electrostatic precipitation. Therefore, a new aerosol generator was developed, consisting of a piezo crystal and a swirl chamber of a particular geometry. Droplets in the lower micrometer size range with narrow size distribution were obtained.

These were subsequently dried, and small particles were formed. The median size of these particles was about 2 μm with a narrow size distribution (span = 1.1) and a submicron share of 10%. This was independent of the drug substance. These particles were then deposited in xylitol as the carrier material using electrostatic precipitation. A 200-fold higher drug content in the carrier material was achieved compared to previous investigations [38]. The three drug substances exhibited different separation behaviors, which was attributed to different charging mechanisms of these compounds.

The presented experimental setup is a versatile tool. This spray dryer is capable of producing uniform particles for different substances and the charging of highly resistive materials was possible. The presented novel technique opens several pharmaceutical applications based on in-situ particle collection, such as the improvement of drug solubility, drug-containing bandages, and pulmonary therapeutic systems.

Acknowledgment

This project was financed by the European Regional Development Fund. Open access funding enabled and organized by Projekt DEAL.

The authors have declared no conflict of interest.

Symbols used

A	[m^2]	area of vibrating surface
A_R	[m^2]	area of the resistor layer
d_p	[m]	droplet diameter
E	[V m^{-1}]	electric field strength
f	[s^{-1}]	excitation frequency
I	[A]	electric current
I_N	[-]	intensity number
j	[A m^{-2}]	current density
Oh	[-]	modified Ohnesorge number
R	[Ω]	ohmic resistance
s	[m]	layer thickness
T	[$^{\circ}\text{C}$]	temperature
U	[V]	applied voltage
ΔU	[V]	voltage drop in the resistor layer
We	[-]	modified Weber number

Greek letters

ρ	[kg m^{-3}]	liquid density
ρ_{el}	[Ωcm]	specific resistance
σ	[N m^{-1}]	surface tension

Abbreviations

CXB	celecoxib
ESP	electrostatic precipitator
MESP	melt electrostatic precipitator
NPX	naproxen
PTN	phenytoin

References

- [1] M. Geranpour, E. Assadpour, S. M. Jafari, *Trends Food. Sci. Technol.* **2020**, *102*, 71–90. DOI: <https://doi.org/10.1016/j.tifs.2020.05.028>
- [2] P. Gibot, M. Casas-Cabanas, L. Laffont, S. Levasseur, P. Carlach, *Nat. Mater.* **2008**, *7*, 741–747. DOI: <https://doi.org/10.1038/nmat2245>
- [3] X. F. Zhou, F. Wang, Y. M. Zhu, Z. P. Liu, *J. Mater. Chem.* **2011**, *21* (10), 3353–3358. DOI: <https://doi.org/10.1039/c0jm03287e>
- [4] S. Pyo, R. Müller, C. Keck, in *Nanoencapsulation Technologies for the Food and Nutraceutical Industries* (Ed: S. M. Jafari), 1st ed., Elsevier, Amsterdam **2017**, 4.
- [5] A. Sosnik, K. P. Seremeta, *Adv. Colloid Interface Sci.* **2015**, *223*, 40–54. DOI: <https://doi.org/10.1016/j.cis.2015.05.003>
- [6] F. Schuster, F. Lomello, *J. Phys.: Conf. Ser.* **2013**, *429*, 012054.
- [7] A. Bitterlich, C. Laabs, E. Busmann, A. Grandeur, M. Juhnke, H. Bunjes, A. Kwade, *Chem. Eng. Technol.* **2014**, *37* (5), 840–846. DOI: <https://doi.org/10.1002/ceat.201300697>
- [8] C. Muehlenfeld, B. Kann, M. Windbergs, M. Thommes, *J. Pharm. Sci.* **2013**, *102* (11), 4132–4139. DOI: <https://doi.org/10.1002/jps.23731>
- [9] J. Möschwitzer, G. Achleitner, H. Pomper, R. H. Müller, *Eur. J. Pharm. Biopharm.* **2004**, *58* (3), 615–619. DOI: <https://doi.org/10.1016/j.ejpb.2004.03.022>
- [10] R. Muller, C. Keck, *Eur. J. Pharm. Biopharm.* **2006**, *62*, 3–16. DOI: <https://doi.org/10.1016/j.ejpb.2005.05.009>
- [11] H. Van de Ven, C. Paulussen, P. B. Feijens, A. Matheussen, P. Rombaut, P. Kayaert, G. Van den Mooter, W. Weyenberg, P. Cos, L. Maes, A. Ludwig, *J. Controlled Release* **2012**, *161* (3), 795–803. DOI: <https://doi.org/10.1016/j.jconrel.2012.05.037>
- [12] Z. H. Loh, A. K. Samanta, P. W. S. Heng, *Asian J. Pharm. Sci.* **2015**, *10* (4), 255–274. DOI: <https://doi.org/10.1016/j.ajps.2014.12.006>
- [13] A. A. Date, V. Patravale, *Curr. Opin. Colloid Interface Sci.* **2004**, *9* (3–4), 222–235. DOI: <https://doi.org/10.1016/j.cocis.2004.06.009>
- [14] H.-K. Chan, P. C. L. Kwok, *Adv. Drug Delivery Rev.* **2011**, *63* (6), 406–416. DOI: <https://doi.org/10.1016/j.addr.2011.03.011>
- [15] S. M. Jafari, C. Arpagaus, M. A. Cerqueira, K. Samborska, *Trends Food Sci. Technol.* **2021**, *109*, 632–646. DOI: <https://doi.org/10.1016/j.tifs.2021.01.061>
- [16] S. Kruger, E. Eichler, L. Strobel, A. Schubert-Unkmeier, K. O. Johswich, *Pathog. Dis.* **2018**, *76* (8), fty086. DOI: <https://doi.org/10.1093/femspd/fty086>
- [17] A. A. Öztürk, C. Arpagaus, *Assay Drug Dev. Technol.* **2021**, *19* (7), 412–441. DOI: <https://doi.org/10.1089/adt.2021.053>
- [18] K. Masters, *Spray Drying Handbook*, 1st ed., George Godwin, London **1985**.
- [19] A. B. D. Nandiyanto, K. Okuyama, *Adv. Powder Technol.* **2011**, *22* (1), 1–19. DOI: <https://doi.org/10.1016/j.appt.2010.09.011>
- [20] P. Walzel, T. Furuta, in *Modern Drying Technology, Vol. 3: Product Quality and Formulation* (Eds: E. Tsotsas, A. S. Mujumdar), Wiley-VCH, Weinheim **2011**, 6.

- [21] R. Strob, A. Dobrowolski, G. Schaldach, P. Walzel, M. Thommes, *Int. J. Pharm.* **2018**, *548* (1), 423–430. DOI: <https://doi.org/10.1016/j.ijpharm.2018.06.067>
- [22] A. Dobrowolski, R. Strob, J. Nietfeld, D. Pieloth, H. Wiggers, M. Thommes, *Int. J. Pharm.* **2018**, *548* (1), 237–243. DOI: <https://doi.org/10.1016/j.ijpharm.2018.06.069>
- [23] S. F. Mause, P. von Hundelshausen, A. Zernecke, R. R. Koenen, C. Weber, *Arterioscler., Thromb., Vasc. Biol.* **2005**, *25* (7), 1512–1518. DOI: <https://doi.org/10.1161/01.ATV.0000170133.43608.37>
- [24] X. Li, N. Anton, C. Arpagaus, F. Belleiteix, T. F. Vandamme, *J. Controlled Release* **2010**, *147* (2), 304–310. DOI: <https://doi.org/10.1016/j.jconrel.2010.07.113>
- [25] S. H. Lee, D. Heng, W. K. Ng, H. K. Chan, R. B. Tan, *Int. J. Pharm.* **2011**, *403* (1–2), 192–200. DOI: <https://doi.org/10.1016/j.ijpharm.2010.10.012>
- [26] K. Schmid, C. Arpagaus, W. Friess, *Pharm. Dev. Technol.* **2011**, *16* (4), 287–294. DOI: <https://doi.org/10.3109/10837450.2010.485320>
- [27] R. Rajan, A. B. Pandit, *Ultrasonics* **2001**, *39* (4), 235–255. DOI: [https://doi.org/10.1016/s0041-624x\(01\)00054-3](https://doi.org/10.1016/s0041-624x(01)00054-3)
- [28] R. J. Lang, *J. Acoust. Soc. Am.* **1962**, *34* (1), 6–8.
- [29] A. A. Barba, M. d'Amore, S. Cascone, G. Lamberti, G. Titomanlio, *Chem. Eng. Process.* **2009**, *48* (10), 1475–1481. DOI: <https://doi.org/10.1016/j.cep.2009.08.004>
- [30] K. A. Ramisetty, A. B. Pandit, P. R. Gogate, *Ultrason. Sonochem.* **2013**, *20* (1), 254–264. DOI: <https://doi.org/10.1016/j.ultsonch.2012.05.001>
- [31] Y. Zhang, S. M. Yuan, L. Z. Wang, *Exp. Therm. Fluid Sci.* **2021**, *120*, 110219. DOI: <https://doi.org/10.1016/j.exptthermflusc.2020.110219>
- [32] R. A. Khaire, P. R. Gogate, *Dry Technol.* **2021**, *39* (12), 1832–1853. DOI: <https://doi.org/10.1080/07373937.2020.1804926>
- [33] K. Ståhl, M. Claesson, P. Lilliehorn, H. Lindén, K. Bäckström, *Int. J. Pharm.* **2002**, *233* (1–2), 227–237.
- [34] Y. F. Maa, P. A. Nguyen, K. Sit, C. C. Hsu, *Biotechnol. Bioeng.* **1998**, *60* (3), 301–309. DOI: [https://doi.org/10.1002/\(SICI\)1097-0290\(19981105\)60:3<301::AID-BIT5>3.0.CO;2-L](https://doi.org/10.1002/(SICI)1097-0290(19981105)60:3<301::AID-BIT5>3.0.CO;2-L)
- [35] M. Maury, K. Murphy, S. Kumar, L. Shi, G. Lee, *Eur. J. Pharm. Biopharm.* **2005**, *59* (3), 565–573. DOI: <https://doi.org/10.1016/j.ejpb.2004.10.002>
- [36] L. W. Chen, E. Gonze, M. Ondarts, J. Outin, Y. Gonthier, *Sep. Purif. Technol.* **2020**, *247*, 116964. DOI: <https://doi.org/10.1016/J.Seppur.2020.116964>
- [37] A. Mizuno, *IEEE Trans. Dielectr. Electr. Insul.* **2000**, *7* (5), 615–624. DOI: <https://doi.org/10.1109/94.879357>
- [38] A. Dobrowolski, D. Pieloth, H. Wiggers, M. Thommes, *Pharmaceutics* **2019**, *11* (6), 276. DOI: <https://doi.org/10.3390/pharmaceutics11060276>
- [39] K. Parker, *Electrical Operation of Electrostatic Precipitators*, 1st ed., Institution of Engineering & Technology, London **2003**.
- [40] H. J. White, *Trans. Am. Inst. Electr. Eng.* **1951**, *70* (2), 1186–1191. DOI: <https://doi.org/10.1109/T-AIEE.1951.5060545>
- [41] M. Majid, H. Wiggers, P. Walzel, in *Proc. ISESP* (Ed: N. Grass), International Society for Electrostatic Precipitation, Birmingham, AL **2011**, 185–190.
- [42] A. Justen, G. Schaldach, M. Thommes, in *Proc. ICLASS* (Eds: M. Linne, M. Marengo, P. Aleiferis), Institute for Liquid Atomization and Spray Systems, Edinburgh, UK **2021**, 92.
- [43] T. Kudo, K. Sekiguchi, K. Sankoda, N. Namiki, S. Nii, *Ultrason. Sonochem.* **2017**, *37*, 16–22. DOI: <https://doi.org/10.1016/j.ultsonch.2016.12.019>
- [44] Y. F. Yano, K. Matsuura, T. Fukazu, F. Abe, A. Wakisaka, H. Kobara, K. Kaneko, A. Kumagai, Y. Katsuya, M. Tanaka, *J. Chem. Phys.* **2007**, *127* (3), 031101. DOI: <https://doi.org/10.1063/1.2754676>
- [45] A. Lozano, S. Jiménez, E. Calvo, J. L. Santolaya, F. Barreras, in *Proc. ICLASS* (Eds: M. Linne, M. Marengo, P. Aleiferis), Institute for Liquid Atomization and Spray Systems, Edinburgh, UK **2021**, 47.
- [46] D. Pieloth, H. Wiggers, P. Walzel, *Chem. Eng. Technol.* **2014**, *37* (4), 627–634. DOI: <https://doi.org/10.1002/ceat.201400012>
- [47] Y. Aleksin, A. Vora, U. Riebel, *Powder Technol.* **2016**, *294*, 353–364. DOI: <https://doi.org/10.1016/j.powtec.2016.02.031>
- [48] U. Riebel, Y. Aleksin, A. Vora, *Chem. Ing. Tech.* **2013**, *85* (3), 235–244. DOI: <https://doi.org/10.1002/cite.201200110>
- [49] M. Majid, A. Rojek, H. Wiggers, P. Walzel, *Chem. Ing. Tech.* **2010**, *82* (12), 2201–2207. DOI: <https://doi.org/10.1002/cite.201000003>
- [50] E. Cereda, G. M. B. Marazzan, M. Pedretti, G. W. Grime, A. Baldacci, *J. Aerosol Sci.* **1996**, *27* (4), 607–619. DOI: [https://doi.org/10.1016/0021-8502\(95\)00571-4](https://doi.org/10.1016/0021-8502(95)00571-4)
- [51] D. Steiner, C. Lanzerstorfer, *Fuel* **2018**, *227*, 59–66. DOI: <https://doi.org/10.1016/j.fuel.2018.04.086>
- [52] P. V. Bush, T. R. Snyder, *Powder Technol.* **1992**, *72* (3), 207–213. DOI: [https://doi.org/10.1016/0032-5910\(92\)80039-Y](https://doi.org/10.1016/0032-5910(92)80039-Y)
- [53] W. Glover, H. K. Chan, *J. Aerosol Sci.* **2004**, *35* (6), 755–764. DOI: <https://doi.org/10.1016/j.jaerosci.2003.12.003>
- [54] M. Rowland, A. Cavocchi, F. Thielmann, J. Kulon, J. Shur, R. Price, *Pharm. Res.* **2019**, *36* (1), 15. DOI: <https://doi.org/10.1007/s11095-018-2544-9>